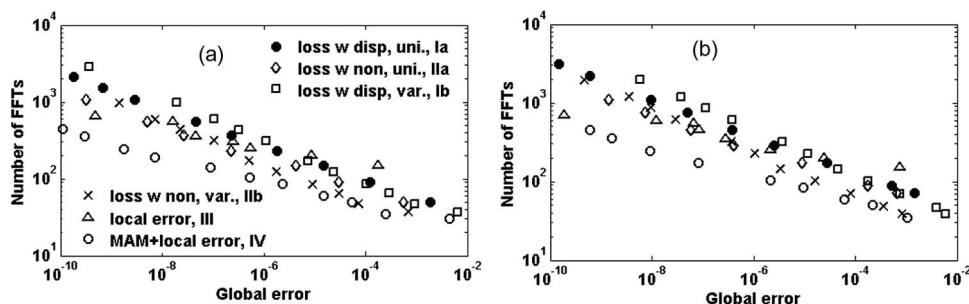


# Comparison of Split-Step Fourier Schemes for Simulating Fiber Optic Communication Systems

Volume 6, Number 4, August 2014

Jing Shao  
Xiaojun Liang  
Shiva Kumar, Member, IEEE



DOI: 10.1109/JPHOT.2014.2340993  
1943-0655 © 2014 IEEE

# Comparison of Split-Step Fourier Schemes for Simulating Fiber Optic Communication Systems

Jing Shao, Xiaojun Liang, and Shiva Kumar, *Member, IEEE*

Department of Electrical and Computer Engineering, McMaster University,  
Hamilton, ON L8S 4L8, Canada

DOI: 10.1109/JPHOT.2014.2340993

1943-0655 © 2014 IEEE. Translations and content mining are permitted for academic research only.

Personal use is also permitted, but republication/redistribution requires IEEE permission.

See [http://www.ieee.org/publications\\_standards/publications/rights/index.html](http://www.ieee.org/publications_standards/publications/rights/index.html) for more information.

Manuscript received June 10, 2014; revised July 14, 2014; accepted July 15, 2014. Date of publication July 18, 2014; date of current version July 31, 2014. Corresponding author: J. Shao (e-mail: jingshao.hust@gmail.com).

**Abstract:** This paper mainly focuses on efficient schemes for simulating propagation in optical fibers. Various schemes based on split-step Fourier techniques to solve the nonlinear Schrödinger equation (NLSE), which describes the propagation in optical fibers, are compared. In general, the schemes in which the loss operator is combined with non-linearity operator are found to be more computationally efficient than the schemes in which the loss is combined with dispersion. When the global error is large, the schemes with variable step size outperform the ones with uniform step size. The schemes based on local error and/or minimum area mismatch (MAM) further improve the computational efficiency. In this scheme, by minimizing the area mismatch between the exponential profile and its stepwise approximation, an optimal step size distribution is found. The optimization problem is solved by the steepest descent algorithm. The number of steps to get the desired accuracy is determined by the local error method. The proposed scheme is found to have higher computational efficiency than the other schemes studied in this paper. For QPSK systems, when the global error is  $10^{-8}$ , the number of fast Fourier transforms (FFTs) needed for the conventional scheme (loss combined with dispersion and uniform step size) is 5.8 times that of the proposed scheme. When the global error is  $10^{-6}$ , the number of FFTs needed for the conventional scheme is 3.7 times that of the proposed scheme.

**Index Terms:** Optical fiber communication modeling, numerical simulation, nonlinear Schrödinger equation (NLSE), split-step Fourier method (SSFM).

## 1. Introduction

The split-step Fourier method (SSFM) is widely used to solve the nonlinear Schrödinger equation (NLSE), which describes the evolution of optical field envelope in optical fibers [1]–[4]. In SSFM, dispersion and nonlinearity operators are assumed to act independently over a small step size. A pair of fast Fourier transforms (FFTs) is used to solve the NLSE when there is only dispersion and/or loss and then, a phase shift is introduced to account for the nonlinear effects when the dispersion is absent. Recently digital back propagation (DBP) has drawn significant attention to mitigate the linear and nonlinear impairments [5]–[11]. In DBP, the NLSE is solved in digital domain with the reversed signs of dispersion, loss and nonlinear coefficients. Therefore, efficient algorithms to solve the NLSE have become even more important.

In solving the NLSE, smaller step size leads to results closer to the exact solution, but it takes more computational time. Thus, there is a trade-off between the accuracy and computational cost. The objective of this paper is to compare the accuracy of various SSFMs for the given computational cost. In the conventional approach [2], the linear operator,  $\hat{D}$  takes into the account of dispersive and loss effects while the nonlinear operator,  $\hat{N}$  takes into account only the Kerr effect. Instead, it is possible to include the loss effect along with the Kerr effect in  $\hat{N}$  and we find that this scheme has higher computational efficiency than the conventional approach. It is because the path-averaged nonlinear phase shift is introduced which takes into account the power attenuation due to fiber loss within the step while in the conventional scheme, nonlinear phase shift is determined by the power at the beginning or the middle of the step. If the losses were to vary with frequency, introducing losses into the nonlinear operator would not be a simple task. For optical waveguides, the losses change across the relevant spectrum of the optical signal and hence, this scheme is not suitable. However, for optical fibers, over the simulation bandwidth, the loss is nearly constant.

In the presence of fiber loss, the uniform step size is not optimum since the nonlinear phase shift accumulated in each step decreases exponentially with distance due to loss. The step size distribution can be optimized using the local error method [4] or minimum area mismatch (MAM) [12]–[14] or the combination of both. Local error method is a powerful technique to solve the NLSE, in which the step size is adaptively chosen so as to bound the relative local error. In MAM, the step size distribution is optimized by minimizing the area mismatch between the exponential curve and its stepwise approximation. In this paper, a novel scheme that combines the merits of local error method and MAM is introduced. Using this approach, the computational efficiency can be improved by a factor 2.5 to 5, and a factor 1.6 to 3.1 as compared to the conventional and local error methods, respectively, when the global error is in the range of practical interest.

## 2. Theory

### 2.1. Principle of the Split-Step Fourier Method (SSFM)

The NLSE is used to describe the optical pulse propagation in fibers. When the pulse width is large ( $> 5$  ps) and the higher order dispersion and the delayed nonlinear response are neglected, the NLSE can be written as

$$\frac{\partial A}{\partial z} = -\frac{\alpha}{2}A - \frac{i}{2}\beta_2 \frac{\partial^2 A}{\partial T^2} + i\gamma|A|^2A \quad (1)$$

where  $A$  is the complex field envelope, and  $\alpha$ ,  $\beta_2$ , and  $\gamma$  are loss coefficient, second order dispersion parameter, and nonlinear coefficient. Equation (1) has an analytical soliton solution for a specific case when  $\beta_2 < 0$ . However, for most cases, it has to be solved numerically. SSFM is extensively used to solve the NLSE numerically. To explain the SSFM clearly, it's convenient to write (1) in the following form:

$$\frac{\partial A}{\partial z} = [\hat{D} + \hat{N}(A)]A. \quad (2)$$

Here,  $\hat{D}$  and  $\hat{N}$  are the operators that account for dispersion and nonlinearity, respectively. If we neglect the fiber loss

$$\hat{D} = -\frac{i}{2}\beta_2 \frac{\partial^2}{\partial T^2}, \quad \hat{N}(A) = i\gamma|A|^2. \quad (3)$$

The cases when the fiber loss is taken into account will be discussed later. In fibers, dispersion and nonlinearity act simultaneously, but they can be roughly treated as being independent in a

very small distance. If the unsymmetric split-step scheme is employed, (2) has an approximate solution as [2]

$$A(z+h, T) \approx \exp(h\hat{D}) \exp\left(\int_z^{z+h} \hat{N}(z') dz'\right) A(z, T). \quad (4)$$

In the symmetric scheme, (2) can be approximated as

$$A(z+h, T) \approx \exp\left(\frac{h}{2}\hat{D}\right) \exp\left(\int_z^{z+h} \hat{N}(z') dz'\right) \exp\left(\frac{h}{2}\hat{D}\right) A(z, T). \quad (5)$$

Equations (4) and (5) are not the exact solutions of (2) since  $\hat{D}$  and  $\hat{N}$  don't commute. Using Baker-Hausdorff formula [15], the dominant error term of (4) is of the order  $h^2$ , and the leading error of (5) is of the order  $h^3$ . Since the symmetric scheme is more accurate than the unsymmetric one, it has been utilized in the numerical calculation throughout this paper. The operation  $\exp(h\hat{D}/2)A(z, T)$  can be realized using a pair of FFTs and hence, the computational cost of a single-step symmetric scheme is approximately twice that of the unsymmetric scheme. However, after multiple steps, the computational cost is approximately the same. This can be seen by dividing the fiber length into  $m$  steps and the optical field envelope after  $m$  steps is obtained by concatenation of operators in (5), [2]

$$A(z+mh, T) \cong \exp\left(\frac{h}{2}\hat{D}\right) \exp\left(ih\gamma|A(z+(m-1)h, T)|^2\right) \exp(h\hat{D}) \exp\left(ih\gamma|A(z+(m-2)h, T)|^2\right) \dots \times \exp(h\hat{D}) \exp\left(ih\gamma|A(z, T)|^2\right) \exp\left(\frac{h}{2}\hat{D}\right) A(z, T). \quad (6)$$

To evaluate (6), we need only  $(m+1)$  FFT pairs since the dispersion operators of the neighboring steps are combined while the unsymmetric scheme requires  $m$  FFT pairs. Throughout this paper, we combine the dispersion operators of the neighboring steps whenever it is feasible, which reduces the computational cost by a factor of 2.

When the fiber loss is included, there are two options. It could be included with dispersion or with nonlinearity. For the first case (see Sections 2.2 and 2.4), (3) is modified as

$$\hat{D}_1 = -\frac{i}{2}\beta_2 \frac{\partial^2}{\partial T^2} - \frac{\alpha}{2}, \quad \hat{N}_1(A) = i\gamma|A|^2. \quad (7)$$

For the latter case, we have (see Sections 2.3 and 2.5)

$$\hat{D}_2 = -\frac{i}{2}\beta_2 \frac{\partial^2}{\partial T^2} \quad (8)$$

$$\hat{N}_2(A) = i\gamma|A|^2 - \frac{\alpha}{2}. \quad (9)$$

The efficiency of the scheme depends on whether the loss is included with dispersion or nonlinearity. Also, the step size distribution can affect the scheme performance. In the following subsections, several schemes of SSFM to solve the NLSE will be reviewed and a novel scheme based on MAM and local error method will be proposed.

## 2.2. Uniform Step Size, Loss With Dispersion (Scheme 1a)

The simplest way to realize the SSFM is to introduce uniform step size, in which the accuracy can be improved by selecting a smaller step size. In scheme 1a, the loss is combined with

dispersion [see (7)]. Using the rectangular rule for the integrals in (4) and (5), they become

$$A(z+h, T) \approx \exp(h\hat{D}_1) \exp\left(ih\gamma|A(z, T)|^2\right) A(z, T) \quad (10)$$

$$A(z+h, T) \approx \exp\left(\frac{h\hat{D}_1}{2}\right) \exp\left(ih\gamma\left|A_{11}\left(z+\frac{h}{2}, T\right)\right|^2\right) \exp\left(\frac{h\hat{D}_1}{2}\right) A(z, T) \quad (11)$$

where  $A_{11}(z+h/2, T) = \exp(h\hat{D}_1/2)A(z, T)$ .

For a certain nonlinear phase rotation  $\phi^{NL}$ , the step size is determined by

$$h = \frac{\phi^{NL}}{\gamma P_{peak}} \quad (12)$$

where  $P_{peak}$  is the peak power of the optical signal launched to a fiber span. The same step size is used in the following steps within the span.

Using the Baker-Hausdorff formular, the leading error term is found to be (see Appendix A)

$$E_I = \left( \frac{i}{24} \beta_2 \gamma^2 |A_{11}|^4 \frac{\partial^2}{\partial T^2} - \frac{i}{12} \beta_2 \gamma^2 |A_{11}|^2 \frac{\partial^2}{\partial T^2} |A_{11}|^2 - \frac{i}{48} \beta_2^2 \gamma \frac{\partial^2}{\partial T^2} |A_{11}|^2 \frac{\partial^2}{\partial T^2} \right. \\ \left. + \frac{i}{96} \beta_2^2 \gamma \frac{\partial^4}{\partial T^4} |A_{11}|^2 + \frac{i}{96} \beta_2^2 \gamma |A_{11}|^2 \frac{\partial^4}{\partial T^4} + \frac{i}{24} \beta_2 \gamma^2 \frac{\partial^2}{\partial T^2} |A_{11}|^4 \right) h^3 A(0, T) \quad (13)$$

### 2.3. Uniform Step Size, Loss With Nonlinearity (Scheme IIa)

This scheme is almost the same as scheme Ia except that the fiber loss is included in  $\hat{N}$  [see Eqs. (8) and (9)]. Let us first ignore the operator  $\hat{D}$  in (2). Using (9) for  $\hat{N}$ , we find

$$\frac{dA}{dz} = \left( i\gamma|A|^2 - \frac{\alpha}{2} \right) A. \quad (14)$$

Let

$$A = |A|e^{i\theta}. \quad (15)$$

Substituting Eq. (15) in Eq. (14) and separating the real and imaginary parts, we find

$$\frac{d|A|}{dz} = -\frac{\alpha}{2}|A| \quad (16)$$

$$\frac{d\theta}{dz} = \gamma|A|^2. \quad (17)$$

Solving Eqs. (16) and (17), we obtain

$$A(z+h, T) = \exp\left(-\frac{\alpha}{2}h + i\gamma h_{eff}|A(z, T)|^2\right) A(z, T) \quad (18)$$

where

$$h_{eff} = \frac{1 - \exp(-\alpha h)}{\alpha}. \quad (19)$$

Therefore, (4) and (5) are modified as

$$A(z+h, T) \approx \exp(h\hat{D}_2) \exp\left(-\frac{\alpha}{2}h + i\gamma h_{\text{eff}}|A(z, T)|^2\right) A(z, T) \quad (20)$$

$$A(z+h, T) \approx \exp\left(\frac{h}{2}\hat{D}_2\right) \exp\left(-\frac{\alpha}{2}h + i\gamma h_{\text{eff}}\left|A_{l2}\left(z+\frac{h}{2}, T\right)\right|^2\right) \exp\left(\frac{h}{2}\hat{D}_2\right) A(z, T) \quad (21)$$

where  $A_{l2}(z+h/2, T) = \exp(h\hat{D}_2/2)A(z, T)$ .

For this scheme, the leading error is found to be (see Appendix A)

$$E_{II} = \left( \frac{i}{24} h_{\text{eff}} \beta_2 \gamma^2 |A_{l2}|^4 \frac{\partial^2}{\partial T^2} - \frac{i}{12} h_{\text{eff}} \beta_2 \gamma^2 |A_{l2}|^2 \frac{\partial^2}{\partial T^2} |A_{l2}|^2 - \frac{i}{48} h \beta_2^2 \gamma \frac{\partial^2}{\partial T^2} |A_{l2}|^2 \frac{\partial^2}{\partial T^2} \right. \\ \left. + \frac{i}{96} h \beta_2^2 \gamma \frac{\partial^4}{\partial T^4} |A_{l2}|^2 + \frac{i}{96} h \beta_2^2 \gamma |A_{l2}|^2 \frac{\partial^4}{\partial T^4} + \frac{i}{24} h_{\text{eff}} \beta_2 \gamma^2 \frac{\partial^2}{\partial T^2} |A_{l2}|^4 \right) h h_{\text{eff}} A(0, T). \quad (22)$$

As we will show later, given the same step size, the performance of the scheme when loss is clubbed with nonlinearity is better than that when loss is with dispersion, especially when the field change due to loss within the interval  $[z, z+h]$  is larger than that due to dispersion. This is because the operator  $\hat{N}_2$  in (21) represents the mean nonlinear phase shift in the interval  $[z, z+h]$  taking into account the power loss in that interval. In contrast, the operator  $\hat{N}_1$  in Eqs. (10) or (11) includes only the power  $|A(z, T)|^2$  at the beginning or the middle of the step and it ignores the nonlinear phase variations within the step due to fiber loss. Although it is possible to set up an iterative procedure to approximate the integrals in (4) and (5) instead of the rectangular rule [2], we have found that the computational efficiency (computational cost for the given accuracy) is lower for the schemes based on the iterative procedure.

#### 2.4. Variable Step Size, Loss With Dispersion (Scheme Ib)

The disadvantage of scheme Ia is that the nonlinear phase accumulated over a step decreases with distance due to fiber loss and the step size determined by the fiber launch power [see (12)] is too small for steps closer to the end of the span. If we ignore the pulse broadening due to dispersion, the peak power decreases exponentially with distance. So, (12) is modified as

$$h_{m+1} = \frac{\phi^{\text{NL}}}{\gamma P_{\text{peak}} e^{-\alpha z_m}}, \quad m = 0, 1, 2, \dots \quad (23)$$

where  $h_m$  is the step size at  $z_m$ ,  $z_0 = 0$  and  $z_m = \sum_{k=1}^m h_k$ . In this scheme, loss is combined with dispersion and,  $\hat{D}$  and  $\hat{N}$  are given by Eqs. (7).

#### 2.5. Variable Step Size, Loss With Nonlinearity (Scheme IIb)

In this scheme, the selection of step size is the same as that of scheme Ib. In each step, loss is combined with nonlinearity, and  $\hat{D}$  and  $\hat{N}$  operators are given by (8) and (9), respectively. This scheme brings both the advantages of loss with nonlinearity and an efficient step size distribution.

#### 2.6. Local-Error Method (Scheme III)

The method developed in [4] is summarized as follows. Suppose the field  $A$  at  $z$  is known. The field at  $z+2h$  can be obtained using (5) as

$$A_c(z+2h) = \exp(h\hat{D}_1) \exp\left(\int_z^{z+2h} \hat{N}_1(z') dz'\right) \exp(h\hat{D}_1) A(z) = A_{\text{exact}}(z+2h) + e_1. \quad (24)$$

For the symmetric SSFM, the error  $e_1$  is of the order  $(2h)^3$  and hence, (24) may be written as

$$A_c(z + 2h) = A_{\text{exact}}(z + 2h) + C(2h)^3 + O(h^4), \quad (25)$$

where  $A_c(z + 2h)$  and  $A_{\text{exact}}(z + 2h)$  represent the coarse and exact solutions at  $z + 2h$ , respectively, and  $C$  is a constant. The solution at  $z + 2h$  can also be obtained by using (5) twice with a step size of  $h$ , which we call the fine solution  $A_f$

$$\begin{aligned} A_f(z + 2h) &= \exp\left(\frac{h}{2}\hat{D}_1\right) \exp\left(\int_{z+h}^{z+2h} \hat{N}_1(z') dz'\right) \exp(h\hat{D}_1) \exp\left(\int_z^{z+h} \hat{N}_1(z') dz'\right) \exp\left(\frac{h}{2}\hat{D}_1\right) A(z) \\ &= A_{\text{exact}}(z + 2h) + e_2 \end{aligned} \quad (26)$$

where the error  $e_2$  is of the order  $2h^3$ . Equation (26) may be rewritten as

$$A_f(z + 2h) = A_{\text{exact}}(z + 2h) + 2Ch^3 + O(h^4). \quad (27)$$

By taking appropriate linear combination of  $A_c$  and  $A_f$ , the term proportional to  $h^3$  can be eliminated so that the leading order error is  $O(h^4)$ , i.e.,

$$A_4(z + 2h) = \frac{4}{3}A_f(z + 2h) - \frac{1}{3}A_c(z + 2h) = A_{\text{exact}}(z + 2h) + O(h^4). \quad (28)$$

$A_4(z + 2h)$  is the solution at  $z + 2h$  with a higher accuracy and used as the input of the next step. The local error in the coarse solution relative to the fine solution is a measure of the relative local error, defined as

$$e = \frac{\|A_f(z + 2h) - A_c(z + 2h)\|^2}{\|A_f(z + 2h)\|^2} \quad (29)$$

and  $\|\cdot\|$  is the norm that equals to  $(\int |\cdot|^2 dt)^{1/2}$ . The main principle of this method is that, given a target local error  $e_{\text{target}}$ , if the current relative local error is larger than the target error, the next step size should be reduced accordingly and vice versa. Although the local-error method introduces additional computational cost while calculating the local error, it's still a very efficient method to control the local error in a certain range, especially when the target global error is very small.

### 2.7. MAM Combined With Local-Error Method (Scheme IV)

In order to further increase the efficiency, we propose a novel scheme by roughly bounding the local error of the first step, fixing the total number of steps  $M$  per span, and then using an optimal distribution of the dispersion operator and nonlinear operator in SSFM. The optimal step size distribution has an elegant feature that the local error within a fiber span has a relatively less variance, so that the local error of the first step is a rough estimate of those of the following steps.

Before describing the novel scheme in detail, we will present the principle and technique to optimize the  $\hat{D}$  and  $\hat{N}$  operator. To explain the method more clearly, it's better to transform the NLSE into its lossless form by the transformation

$$A(z, T) = e^{-\alpha z/2} U(z, T) \quad (30)$$

to obtain

$$\frac{\partial U}{\partial z} = -\frac{i}{2}\beta_2 \frac{\partial^2 U}{\partial T^2} + i\gamma'|U|^2 U \quad (31)$$

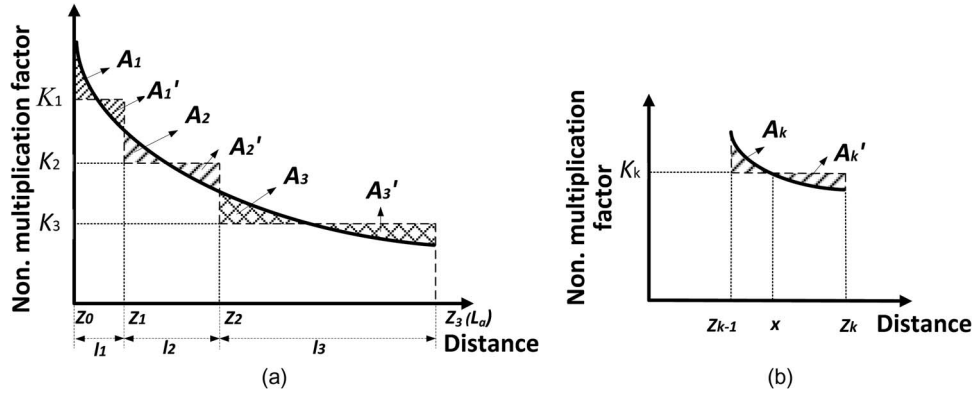


Fig. 1. Stepwise approximation of the effective nonlinear coefficient. (a) The case when  $M=3$ . (b) The general case.  $A_j$  and  $A'_j$  denote area mismatch of the  $j$ th section.

where

$$\gamma' = \gamma \exp(-\alpha z). \quad (32)$$

$\gamma'$  is the effective nonlinear coefficient that exponentially decreases with the distance. In the numerical methods like SSFM, the efficient way is to divide the fiber into several segments with fixed dispersion and effective nonlinear coefficients. As a result, the effective nonlinear coefficient is an approximated stepwise nonlinearity-decreasing curve instead of an ideal exponential one. If the total number of steps  $M$  is sufficiently large, these two curves will almost coincide. Define the nonlinear multiplication factor  $K_j, j = 1, 2, \dots, M$ , for each step, and the stepwise effective nonlinear coefficient is

$$\gamma'_j = K_j \gamma. \quad (33)$$

Fig. 1(a) shows the ideal exponential curve and its stepwise approximation ( $K_j$ ) as a function of distance for  $M = 3$ , and Fig. 1(b) shows a more general case for the  $k$ th step. The split-step algorithm may be written as

$$U(z + l_j) = \exp\left(\frac{l_j}{2} \hat{D}_2\right) \exp\left(i K_j \gamma \left| U_l\left(z + \frac{l_j}{2}\right) \right|^2 l_j\right) \exp\left(\frac{l_j}{2} \hat{D}_2\right) U(z) \quad (34)$$

where  $U_l(z + l_j/2) = \exp(i l_j \hat{D}_2/2) \cdot U(z)$ . We have  $2M - 1$  adjustable parameters, namely,  $K_1, K_2, \dots, K_M$  and  $l_1, l_2, \dots, l_{M-1}$ . The parameters could be so chosen that the global error is minimum. Alternatively, these parameters can be determined using the MAM technique [12]–[14]. In Section 3, it will be shown that the optimum step size determined using the minimum area mismatch technique minimizes the global error, for the case of  $M = 2$ . In Fig. 1(a), the absolute area mismatch between the area under the ideal exponential curve (solid line) and its stepwise approximation (dashed line) is  $\chi = \sum_{j=1}^3 (A_j + A'_j)$  with  $A_j > 0$  and  $A'_j > 0$ .  $l_j$  and  $K_j$  are so chosen that the total area under the exponential curve should be the same as that under its stepwise approximation curve and the area mismatch  $\chi$  should be minimum. So, we have

$$\int_0^{L_a} \exp(-\alpha z) dz = \sum_{j=1}^M K_j l_j. \quad (35)$$

Equation (35) states that the total nonlinear phase shift accumulated over a span of length  $L_a$  should be equal to the sum of the nonlinear phase shifts in each step  $l_j$ . This is an optimization



problem with  $2M - 2$  parameters. The number of parameters can be reduced by a factor of 2 if we impose a constraint that  $K_j$  is the mean of exponential function in the segment  $l_j$ , i.e.,

$$K_j = \frac{1}{l_j} \int_{z_{j-1}}^{z_j} \exp(-\alpha z) dz = \frac{\exp(-\alpha z_{j-1}) - \exp(-\alpha z_j)}{\alpha l_j} \quad (36)$$

where

$$z_j = \sum_{k=1}^j l_k \quad (37)$$

$z_0 = 0$ ,  $z_M = L_a$ , and  $L_a$  is the fiber span length. Now, we consider the optimization problem with  $M - 1$  unknown parameters ( $z_j, j = 1, 2, \dots, M - 1$ ) with the condition that  $\chi$  should be minimum. We solve this problem using the steepest descent algorithm [16]. In Fig. 1(b), let  $x$  be the distance at which the exponential curve and its stepwise approximation line intersect. So, we have

$$K_k = \exp(-\alpha x). \quad (38)$$

The area mismatch  $A_k$  and  $A'_k$  are given by

$$A_k = \frac{e^{-\alpha z_{k-1}} - K_k}{\alpha} - K_k(x - z_{k-1}) \quad (39)$$

$$A'_k = K_k(z_k - x) - \frac{K_k - e^{-\alpha z_k}}{\alpha}. \quad (40)$$

Using (36), we have  $A_k = A'_k$ .

We randomly choose an initial set of  $z_k$ ,  $k = 1, 2, \dots, M - 1$ , and iteratively update the value of every  $z_k$  towards the inverse gradient direction until the optimum points are reached. So, taking the derivative of the total mismatch area  $\chi$  with respect to  $z_k$ , we find

$$\begin{aligned} \frac{\partial \chi}{\partial z_k} = & 2 \left( \frac{\ln K_k}{\alpha} + z_{k-1} \right) \left[ \frac{e^{-\alpha z_k}}{z_k - z_{k-1}} - \frac{e^{-\alpha z_{k-1}} - e^{-\alpha z_k}}{\alpha(z_k - z_{k-1})^2} \right] \\ & + 2 \left( \frac{\ln K_{k+1}}{\alpha} + z_k \right) \left[ -\frac{e^{-\alpha z_k}}{z_{k+1} - z_k} + \frac{e^{-\alpha z_k} - e^{-\alpha z_{k+1}}}{\alpha(z_{k+1} - z_k)^2} \right] - 2e^{-\alpha z_k} + 2K_{k+1}. \end{aligned} \quad (41)$$

Then use the following iterative procedure to update  $z_k$

$$z_k^{(n+1)} = z_k^{(n)} - \frac{\partial \chi}{\partial z_k} \Delta_k, \quad k = 1, 2, \dots, M - 1 \quad (42)$$

where  $z_k^{(n)}$  is the value of  $z_k$  in the  $n$ th iterative step and  $\Delta_k$  is the step size of the steepest descent algorithm. Once the optimum values of  $z_k$  are found, (36) and (37) can be used to obtain the best distribution of the nonlinear multiplication factor  $K_j$  and the segment length  $l_j$ .

The constraint of (36) is not really essential. If we do not impose this constraint, computational complexity of the steepest descent algorithm increases roughly by a factor of 2. However, the improvement in accuracy (in terms of global error) is only marginal and hence, the simulation results of Section 3 are obtained by imposing the constraint of (36).

The steepest descent algorithm converges quickly and Table 1 shows the look-up table for the optimum segment lengths when  $\alpha = 0.2$  dB/km and  $L_a = 80$  km. One of the advantages of this method is that the optimum segment lengths neither depend on the launch power nor on the nonlinear coefficient. Once the look-up table such as that shown in Table 1 is made for a particular fiber type, it can be used for a range of launch powers and other system parameters. Using (34), the optical field at the end of the link can be calculated for the given  $M$ . However,  $M$

TABLE 1

Look-up table for the optimal step size distribution  $\alpha = 0.2$  dB/km,  $L_a = 80$  km

Length (km)	M=2	M=3	M=4	M=5	M=6	M=7	M=8
$l_1$	24.4	14.5	10.4	8.06	6.59	5.58	4.84
$l_2$	55.6	21.8	13.6	9.88	7.77	6.40	5.45
$l_3$	--	43.7	19.8	12.8	9.46	7.51	6.23
$l_4$	--	--	36.3	18.1	12.1	9.08	7.27
$l_5$	--	--	--	31.1	16.8	11.5	8.73
$l_6$	--	--	--	--	27.3	15.6	10.9
$l_7$	--	--	--	--	--	24.3	14.6
$l_8$	--	--	--	--	--	--	22.0

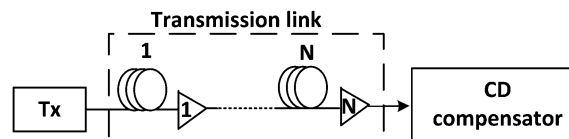


Fig. 2. Schematic of a fiber-optic transmission system.

is undetermined. To relate  $M$  with the desired accuracy, we introduce a technique that combines the local error method with the MAM.

Given an initial  $M$  and a target local error  $e_{\text{target}}$ , calculate the relative local error for the first step  $e_1$  by (29). If  $e_1$  is larger than  $10e_{\text{target}}$ ,  $M$  will be updated by  $2M$ . Else if  $e_1$  is larger than  $e_{\text{target}}$  and less than or equal to  $10e_{\text{target}}$ , then  $M$  will be replaced by  $\lceil 2^{1/3}M \rceil$ . Here,  $\lceil x \rceil$  rounds the element of  $x$  to the nearest integer towards infinity. If  $e_1$  is less than or equal to  $e_{\text{target}}/10$ ,  $M$  will be decreased to  $\lfloor M/2^{1/3} \rfloor$ , where  $\lfloor x \rfloor$  rounds the element of  $x$  to the nearest integer towards minus infinity. Finally, if  $e_1$  is in the target range which is  $(e_{\text{target}}/10, e_{\text{target}}]$ , that  $M$  will be used to find the optimal parameters in the look-up table, which will be used to model the pulse propagation.

In our scheme, the local error for each step will not have a large fluctuation since the step size distribution is optimized for every  $M$ . As a result, we can roughly bound the local error by controlling that of the first step. The implementation for our scheme is different from the local-error method in that we find the total number of steps as well as the step size distribution at the very beginning, instead of adjusting the step size along the fiber length, which saves the computational cost. Since we can combine the dispersion operator [the same way as in (6)] of the neighboring steps, the computational cost can further be reduced by a factor of 2. We will discuss the simulation results in the later section. Since we do not make any assumptions about the system configuration, or the modulation format of the signal, this scheme is system independent and can be widely used for various cases with high efficiency.

### 3. Comparison of Schemes

In this section, we compare the performance of the different schemes described in Section 2 of the SSFM. The system schematic is shown in Fig. 2, which includes a transmitter, a fiber-optic link consisting of  $N$  spans of fibers and amplifiers, and a chromatic dispersion (CD) compensator. The amplifier compensates for the fiber loss exactly, without adding noise. Before implementing the schemes, we simulate a signal propagation in the fiber by the split-step method using a very small step size with the nonlinear phase accumulated per step of 0.00001 radians,

TABLE 2

Single-step error versus step size

h (km)	10 Gbaud		25 Gbaud	
	Single-step error (scheme I)	Single-step error (scheme II)	Single-step error (scheme I)	Single-step error (scheme II)
0.5	1.29e-15	3.43e-17	5.38e-15	4.69e-15
1	8.05e-14	2.15e-15	3.39e-13	2.96e-13
2	5.01e-12	1.33e-13	2.17e-11	1.89e-11
5	1.05e-9	2.85e-11	5.07e-9	4.48e-9
10	5.45e-8	1.45e-9	2.86e-7	2.50e-7
20	2.22e-6	6.10e-8	9.41e-6	7.76e-6
25	6.87e-6	1.88e-7	2.16e-5	1.77e-5
30	1.68e-5	4.59e-7	3.94e-5	3.57e-5
40	6.12e-5	1.73e-6	1.02e-4	1.19e-4
50	1.53e-4	4.46e-6	2.26e-4	2.74e-4
60	3.07e-4	9.79e-6	4.14e-4	4.34e-4

such that the fiber output is very close to the exact solution of NLSE. This output is the reference signal with which we compare the outputs of various schemes. Then, using the same fiber input signal as that used to obtain the reference signal, NLSE is solved by different schemes, and the accuracy and the computational cost are compared. To measure the accuracy, we define the global error by

$$e_{\text{global}} = \frac{\|A_n - A_{\text{ref}}\|^2}{\|A_{\text{ref}}\|^2} \quad (43)$$

where  $A_n$  is the numerical result for scheme  $n$ , and  $A_{\text{ref}}$  is the reference signal. Note that we use the square of the norm instead of the norm itself in (43). We use the number of FFTs as a measure of computational cost since the computational time is roughly proportional to the number of FFTs.

At first, we simulate a fiber-optic system shown in Fig. 2 for 32 quadrature amplitude modulation (QAM) at a symbol rate 25 Gbaud. The following parameters are used throughout this paper unless otherwise specified. A random symbol sequence consisting of 8192 raised-cosine pulses with a roll-off factor of 0.8 is launched to the fiber. The fiber-optic link consists of 10 fiber spans, each 80 km long, and 10 amplifiers. The parameters of the fibers are as follows, the loss coefficient  $\alpha = 0.046 \text{ km}^{-1}$ , the dispersion parameter  $\beta_2 = 5 \text{ ps}^2/\text{km}$ , and the nonlinear coefficient  $\gamma = 2.2 \text{ W}^{-1}\text{km}^{-1}$ . We employed different schemes in Section 2 to carry out the SSFM. After that, a CD compensator is introduced right after the fiber link. Finally, the global error of each scheme is calculated using (43).

Table 2 shows the error in a single step for 10 Gbaud and 25 Gbaud systems, respectively. When the loss is combined with nonlinearity (scheme IIa or b), the single-step error is significantly lower for 10 Gbaud as compared to the case when the loss is combined with dispersion (scheme Ia or b). However, for 25 Gbaud, scheme II has a lower error only when  $h < 40 \text{ km}$ . When  $h$  is larger, scheme II does not perform better because of larger variation of the optical field within the step size due to dispersion.

Fig. 3(a) and (b) show the computational cost (in units of number of FFTs) as a function of the global error for schemes Ia, IIa, Ib, and IIb when the fiber launch power is 0 dBm and 3 dBm, respectively. As can be seen, when the global error is greater than  $10^{-7}$ , scheme IIb (loss combined with nonlinearity and variable step size) is the most efficient scheme of the four schemes. When the global error is large, it corresponds to small number of steps. In this case, uniform

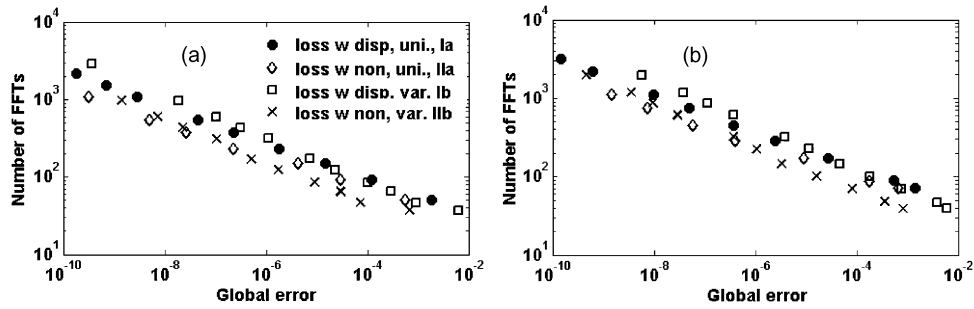


Fig. 3. Plot of the number of FFTs vs global error of the 32QAM system for the schemes Ia, IIa, Ib, and IIb. (a) 0 dBm and (b) 3 dBm.

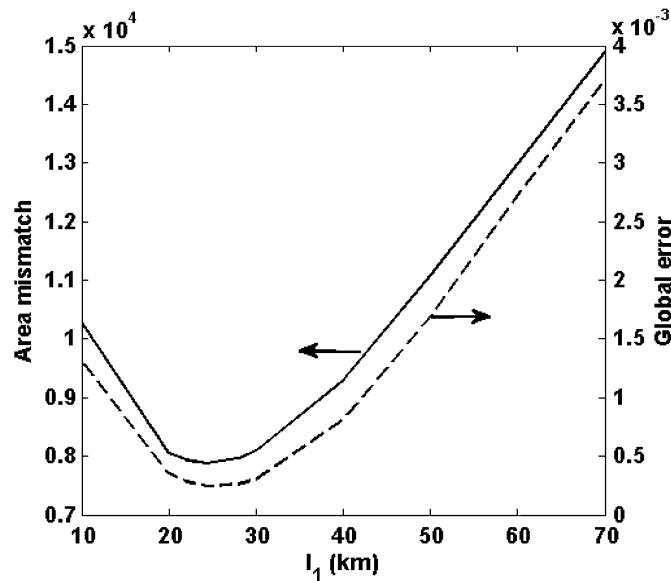


Fig. 4. Area mismatch vs  $l_1$  and global error vs  $l_1$  for the case when  $M = 2$ , launch power = 0 dBm.

step size is not a good choice because the nonlinear phase shift accumulated in a low power region is small and the step size is unnecessarily large wasting the computational resources. When the global error is  $10^{-5}$ , the number of FFTs required for scheme IIb is reduced by a factor of 2 as compared to scheme Ia when the launch power equals to 0 dBm. However, when the global error is less than  $10^{-7}$ , scheme IIa (loss combined with nonlinearity and uniform step size) is the most efficient scheme of the four schemes and it is marginally better than scheme IIb. In either case, schemes in which loss is combined with nonlinearity (schemes IIa and b) outperform the schemes in which the loss is combined with dispersion (schemes Ia and b). For the simulation of fiber-optic transmission system, the region of most practical interest corresponds to a global error in the range of  $10^{-8} - 10^{-2}$ . Typically, practical power of telecom systems range from  $-6$  dBm to 3 dBm depending on the reach and modulation format. The purpose of simulations with higher power (3 dBm) is to evaluate the effect of stronger nonlinear effect in various schemes.

Fig. 4 shows the area mismatch and global error [calculated using (43)] as a function of  $l_1$ , for  $M = 2$ . As can be seen, the value of  $l_1$  that minimizes the area mismatch ( $\chi$ ) also corresponds to minimum global error.

Next, we consider the performance of the local error method (scheme III) and MAM combined with local error method (scheme IV). The results are shown in Fig. 5(a) and (b). Scheme III

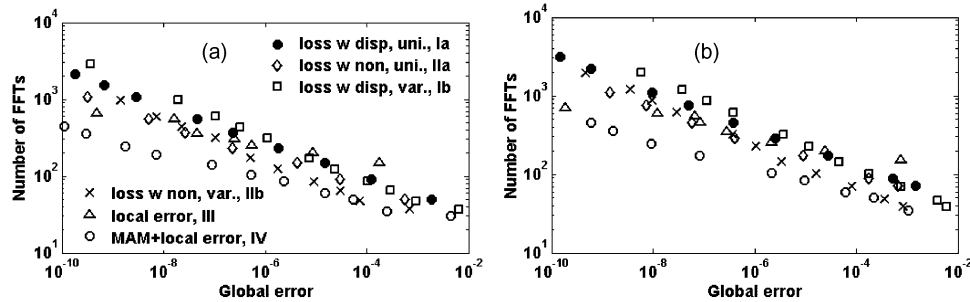


Fig. 5. Plot of the number of FFTs vs global error of the 32QAM system for the schemes I-IV. (a) 0 dBm and (b) 3 dBm.

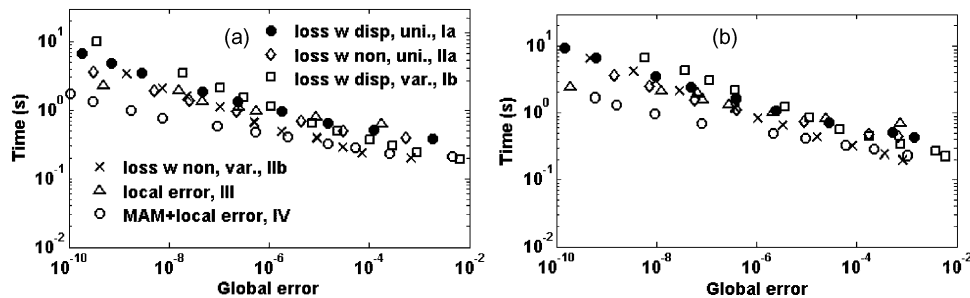


Fig. 6. Plot of the time vs global error of the 32QAM system for the schemes I-IV. (a) 0 dBm and (b) 3 dBm.

gives a better performance than the schemes Ia, IIa, Ib, and IIb when the global error is less than  $10^{-8}$ , and it has a flatter slope, which means the required additional computational cost to achieve a smaller error is the minimum. However, when the global error is large ( $> 10^{-8}$ ), the local error method is not efficient. Similar results are found in [4] in which the efficiency of the local error method is comparable to the other schemes when the global error is large. Fig. 5(a) and (b) show that the MAM combined with local error method is the most efficient one in that, for obtaining the same error, it needs the least number of FFTs. In Fig. 5(a), when the global error is  $10^{-8}$ , the number of FFTs needed for scheme Ia is 4.4 times that of scheme IV, and the number of FFTs required for scheme III is 3.1 that of scheme IV. When the global error is  $10^{-6}$ , the number of FFTs needed for scheme Ia is 2.7 times that of scheme IV and the number of FFTs required for scheme III is 2.5 times that of scheme IV. Comparing Fig. 5(a) and (b), we find that the proposed scheme is the most efficient scheme even at higher launch power. Fig. 6 shows the computational time as a function of the global error. Comparing Figs. 5 and 6, we find that the number of FFTs is a good measure of the computational cost.

Fig. 7 shows the relative local error as a function of distance when the launch power is 0 dBm and the number of steps per span is 5. Dashed and solid lines in Fig. 7 show the results for the case of uniformly distributed step size (scheme Ia) and an optimally distributed step size using MAM (scheme IV), respectively. Both curves show a periodic characteristic due to the system configuration. When the uniformly distributed step size is utilized, the local error is the maximum at the beginning and decreases with distance in each span. This is because the accumulated nonlinear phase per step decreases exponentially with distance in each span due to fiber loss and, smaller accumulated nonlinear phase leads to a more accurate result. In the case when the step size is distributed through the MAM technique, the nonlinear phase accumulated is optimized such that the local error will be smaller and has less variation. From Fig. 7, we see that the local error fluctuation for scheme IV is about one or two orders of magnitude smaller than that for scheme Ia.

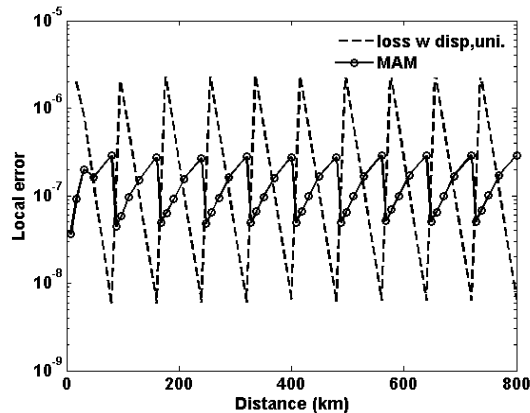


Fig. 7. Local error as a function of distance for schemes Ia and IV for 32QAM system when the launch power is 0 dBm and the number of steps per span  $M = 5$ .

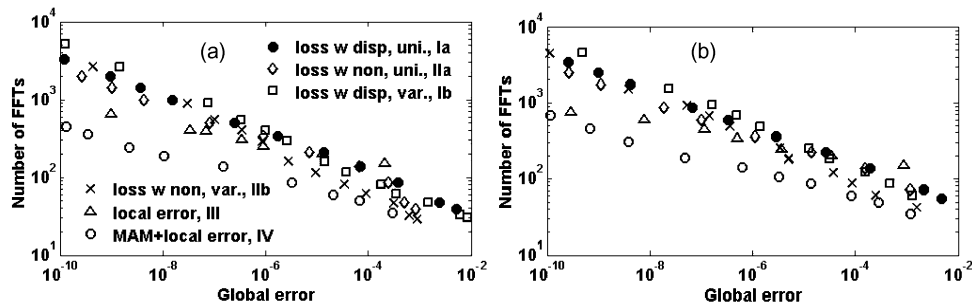


Fig. 8. Plot of the number of FFTs vs global error of the QPSK system for the schemes I-IV. (a) 0 dBm and (b) 3 dBm.

As a next example, we have simulated a fiber-optic system based on quadrature phase shift keying (QPSK). The system configuration and all the parameters of the system are the same as the previous ones. Fig. 8 shows the number of FFTs as a function of global error for all the schemes. Fig. 8(a) and (b) are obtained when the launch power is 0 dBm and 3 dBm, respectively. In Fig. 8(a), when the global error is  $10^{-8}$ , numbers of FFTs needed for scheme Ia and scheme III are 5.8 and 2.5 times that of scheme IV, respectively. When the global error is  $10^{-6}$ , the numbers of FFTs required for scheme Ia and scheme III are 3.7 and 2.4 times that of scheme IV, respectively. Similar results are obtained when the launch power is 3 dBm [see Fig. 8(b)].

#### 4. Conclusion

In this paper, we have studied various schemes using SSFM to solve the NLSE for a fiber-optic system based on two different modulation formats and compared their performances. We proposed a novel scheme combining the local error method with the method based on minimum area mismatch (MAM). The optimum step size for the given number of steps ( $M$ ) is found by minimizing the area mismatch between the exponential curve and its stepwise approximation. The steepest descent algorithm is used for this optimization. The number of steps to have the desired accuracy is determined using the local error method. The advantage of this scheme is that the local error is not calculated at each step which saves the computational cost. The step size distribution is pre-determined by the steepest descent algorithm so that the dispersion operators of the neighboring steps can be combined. The simulation results show that the proposed scheme outperforms the other schemes.

In general, the schemes in which the fiber loss is combined with nonlinearity have higher computational efficiency than the schemes in which the fiber loss is combined with dispersion. When the global error is large ( $> 10^{-7}$ ), the schemes with variable step size outperform the schemes with uniform step size. As for the local error method, it has a flatter slope and outperforms the schemes with uniform or variable step size distribution, especially when the global error is very small.

## Appendix A

The derivation of the error per step for scheme I and II is as follows. The Baker-Hausdorff formula for two noncommuting operators  $\hat{a}$  and  $\hat{b}$  is [2]

$$\exp(\hat{a})\exp(\hat{b}) = \exp\left(\hat{a} + \hat{b} + \frac{1}{2}[\hat{a}, \hat{b}] + \frac{1}{12}[\hat{a} - \hat{b}, [\hat{a}, \hat{b}]] + \dots\right) \quad (\text{A.1})$$

where  $[\hat{a}, \hat{b}] = \hat{a}\hat{b} - \hat{b}\hat{a}$ . By using the Baker-Hausdorff formula twice, we obtain

$$\exp\left(\frac{\hat{a}}{2}\right)\exp(\hat{b})\exp\left(\frac{\hat{a}}{2}\right) = \exp\left(\hat{a} + \hat{b} + \frac{1}{12}\hat{b}\hat{b}\hat{a} - \frac{1}{6}\hat{b}\hat{a}\hat{b} + \frac{1}{12}\hat{a}\hat{b}\hat{a} - \frac{1}{24}\hat{a}\hat{a}\hat{b} - \frac{1}{24}\hat{b}\hat{a}\hat{a} + \frac{1}{12}\hat{a}\hat{b}\hat{b}\right). \quad (\text{A.2})$$

Let us set the right hand side of (A.2) equal to  $\exp(H + E)$ , where

$$H = \hat{a} + \hat{b} \quad (\text{A.3})$$

$$E = \frac{1}{12}\hat{b}\hat{b}\hat{a} - \frac{1}{6}\hat{b}\hat{a}\hat{b} + \frac{1}{12}\hat{a}\hat{b}\hat{a} - \frac{1}{24}\hat{a}\hat{a}\hat{b} - \frac{1}{24}\hat{b}\hat{a}\hat{a} + \frac{1}{12}\hat{a}\hat{b}\hat{b}. \quad (\text{A.4})$$

In the symmetric SSFM, let

$$\hat{a} = h\hat{D}, \quad \hat{b} = h\hat{N}. \quad (\text{A.5})$$

From (A.4), we find that  $E \propto h^3$ . Using Taylor expansion, we find

$$\begin{aligned} \exp(H + E) &= 1 + (H + E) + \frac{(H + E)^2}{2!} + \frac{(H + E)^3}{3!} + \dots \\ &= \left(1 + H + \frac{H^2}{2!} + \frac{H^3}{3!}\right) + \left[E + \frac{1}{2}(E^2 + HE + EH) \right. \\ &\quad \left. + \frac{1}{6}(E^3 + HE^2 + H^2E + EH^2 + E^2H + HEH + EHE)\right] + \dots \\ &\approx \exp(H) + E + O(h^4). \end{aligned} \quad (\text{A.6})$$

In (A.6),  $E$  is  $O(h^3)$  and the higher order terms such as  $E^2$  and  $HE$  are  $O(h^6)$  and  $O(h^4)$ , respectively. So the leading error term for symmetric SSFM is  $E$ . When loss is with dispersion (scheme I)

$$\hat{a}_1 = \hat{D}_1 h = \left(-\frac{i}{2}\beta_2 \frac{\partial^2}{\partial T^2} - \frac{\alpha}{2}\right) h \quad (\text{A.7})$$

$$\hat{b}_1 = \hat{N}_1 h = i\gamma|A_{11}|^2 h \quad (\text{A.8})$$

and the leading error is

$$\begin{aligned}
 E_I &= \left( \frac{1}{12} \hat{b}_1 \hat{b}_1 \hat{a}_1 - \frac{1}{6} \hat{b}_1 \hat{a}_1 \hat{b}_1 + \frac{1}{12} \hat{a}_1 \hat{b}_1 \hat{a}_1 - \frac{1}{24} \hat{a}_1 \hat{a}_1 \hat{b}_1 - \frac{1}{24} \hat{b}_1 \hat{a}_1 \hat{a}_1 + \frac{1}{12} \hat{a}_1 \hat{b}_1 \hat{b}_1 \right) A(0, T) \\
 &= \left( \frac{i}{24} \beta_2 \gamma^2 |A_{I1}|^4 \frac{\partial^2}{\partial T^2} - \frac{i}{12} \beta_2 \gamma^2 |A_{I1}|^2 \frac{\partial^2}{\partial T^2} |A_{I1}|^2 - \frac{i}{48} \beta_2^2 \gamma \frac{\partial^2}{\partial T^2} |A_{I1}|^2 \frac{\partial^2}{\partial T^2} \right. \\
 &\quad \left. + \frac{i}{96} \beta_2^2 \gamma \frac{\partial^4}{\partial T^4} |A_{I1}|^2 + \frac{i}{96} \beta_2^2 \gamma |A_{I1}|^2 \frac{\partial^4}{\partial T^4} + \frac{i}{24} \beta_2 \gamma^2 \frac{\partial^2}{\partial T^2} |A_{I1}|^4 \right) h^3 A(0, T). \quad (\text{A.9})
 \end{aligned}$$

When loss is with nonlinearity (scheme II), let

$$\hat{a}_2 = \hat{D}_2 h = -\frac{i}{2} h \beta_2 \frac{\partial^2}{\partial T^2} \quad (\text{A.10})$$

$$\hat{b}_2 = -\frac{\alpha}{2} h + i \gamma h_{\text{eff}} |A_{I2}|^2 \quad (\text{A.11})$$

and the leading error now is

$$\begin{aligned}
 E_{II} &= \left( \frac{1}{12} \hat{b}_2 \hat{b}_2 \hat{a}_2 - \frac{1}{6} \hat{b}_2 \hat{a}_2 \hat{b}_2 + \frac{1}{12} \hat{a}_2 \hat{b}_2 \hat{a}_2 - \frac{1}{24} \hat{a}_2 \hat{a}_2 \hat{b}_2 - \frac{1}{24} \hat{b}_2 \hat{a}_2 \hat{a}_2 + \frac{1}{12} \hat{a}_2 \hat{b}_2 \hat{b}_2 \right) A(0, T) \\
 &= \left( \frac{i}{24} h_{\text{eff}} \beta_2 \gamma^2 |A_{I2}|^4 \frac{\partial^2}{\partial T^2} - \frac{i}{12} h_{\text{eff}} \beta_2 \gamma^2 |A_{I2}|^2 \frac{\partial^2}{\partial T^2} |A_{I2}|^2 - \frac{i}{48} h \beta_2^2 \gamma \frac{\partial^2}{\partial T^2} |A_{I2}|^2 \frac{\partial^2}{\partial T^2} \right. \\
 &\quad \left. + \frac{i}{96} h \beta_2^2 \gamma \frac{\partial^4}{\partial T^4} |A_{I2}|^2 + \frac{i}{96} h \beta_2^2 \gamma |A_{I2}|^2 \frac{\partial^4}{\partial T^4} + \frac{i}{24} h_{\text{eff}} \beta_2 \gamma^2 \frac{\partial^2}{\partial T^2} |A_{I2}|^4 \right) h h_{\text{eff}} A(0, T). \quad (\text{A.12})
 \end{aligned}$$

## References

- [1] R. H. Hardin and F. D. Tappert, "Application of the split-step Fourier method to the numerical solution of nonlinear and variable coefficient wave equations," *SIAM Rev. Chronicle*, vol. 15, p. 423, 1973.
- [2] G. P. Agrawal, *Nonlinear Fiber Optics*, 5th ed. Oxford, U.K.: Academic, 2013.
- [3] G. Bosco *et al.*, "Suppression of spurious tones induced by the split-step method in fiber systems simulation," *IEEE Photon. Technol. Lett.*, vol. 12, no. 5, pp. 489–491, May 2000.
- [4] O. V. Sinkin, R. Holzlöhner, J. Zweck and C. R. Menyuk, "Optimization of the split-step fourier method in modeling optical-fiber communications systems," *J. Lightw. Technol.*, vol. 21, no. 1, pp. 61–68, Jan. 2003.
- [5] X. Li *et al.*, "Electronic post-compensation of WDM transmission impairments using coherent detection and digital signal processing," *Opt. Exp.*, vol. 16, no. 2, pp. 880–888, Jan. 2008.
- [6] E. Ip and J. Kahn, "Compensation of dispersion and nonlinear impairments using digital backpropagation," *J. Lightw. Technol.*, vol. 26, no. 20, pp. 3416–3425, Oct. 15, 2008.
- [7] E. Ip, "Nonlinear compensation using backpropagation for polarization-multiplexed transmission," *J. Lightw. Technol.*, vol. 28, no. 6, pp. 939–951, Mar. 15, 2010.
- [8] E. Mateo, F. Yaman and G. Li, "Efficient compensation of inter-channel nonlinear effects via digital backward propagation in WDM optical transmission," *Opt. Exp.*, vol. 18, no. 14, pp. 15 144–15 154, Jul. 2010.
- [9] L. B. Du and A. J. Lowery, "Improved single channel backpropagation for intra-channel fiber nonlinearity compensation in long-haul optical communication system," *Opt. Exp.*, vol. 18, no. 16, pp. 17 075–17 088, Aug. 2010.
- [10] R. Asif, C.-Y. Lin, M. Holtmannspoetter, and B. Schmauss, "Optimized digital backward propagation for phase modulated signals in mixed-optical fiber transmission link," *Opt. Exp.*, vol. 18, no. 22, pp. 22 796–22 807, Oct. 2010.
- [11] F. Yaman and G. Li, "Nonlinear impairment compensation for polarization-division multiplexed WDM transmission using digital backward propagation," *IEEE Photon. J.*, vol. 2, no. 5, pp. 816–832, Aug. 2010.
- [12] W. Forsyia, F. M. Knox, and N. J. Doran, "Average soliton propagation in periodically amplified systems with stepwise dispersion-profile fiber," *Opt. Lett.*, vol. 19, no. 3, pp. 174–176, Feb. 1994.
- [13] S. Kumar and J. Shao, "Optical back propagation with optimal step size for fiber optic transmission systems," *IEEE Photon. Technol. Lett.*, vol. 25, no. 5, pp. 523–526, Mar. 2013.
- [14] J. Shao, S. Kumar, and X. Liang, "Digital back propagation with optimal step size for polarization multiplexed transmission," *IEEE Photon. Technol. Lett.*, vol. 25, no. 23, pp. 2327–2330, Dec. 2013.
- [15] G. H. Weiss and A. A. Maradudin, "The Baker-Hausdorff formula and a problem in crystal physics," *J. Math. Phys.* vol. 3, no. 4, pp. 771–777, Jul. 1962.
- [16] S. Haykin, *Adaptive Filter Theory*, 4th ed. Upper Saddle River, NJ, USA: Prentice Hall, 2002.